Astron. Astrophys. 332, 194–198 (1998)

ASTRONOMY
AND
ASTROPHYSICS

A search for gamma rays above 0.5 TeV from the southern radio pulsar PSR1706−44

G.P. Rowell[1,⋆], **S.A. Dazeley**[1], **P.G. Edwards**[2], **J.R. Patterson**[1], **and G.J. Thornton**[1]

[1] Department of Physics and Mathematical Physics, University of Adelaide, Australia, 5005
[2] Institute for Space and Astronautical Science, 3-1-1 Yoshinodai Sagamihara, Kanagawa 229, Japan

Received 28 July 1997 / Accepted 20 November 1997

Abstract. A search for TeV γ-rays from the isolated pulsar PSR1706−44 using the ground-based atmospheric Čerenkov imaging technique has been carried out. Analysis of data taken during 1993 and 1994 from the University of Adelaide's 37 pixel Čerenkov imaging telescope, with special attention paid to the effects of sky-noise differences between ON and OFF source regions, yielded an upper limit to the steady TeV γ-ray emission. The 3σ upper limit for energies above 0.5 TeV is $7.0(\pm 0.7) \times 10^{-11}$ photons cm^{-2}s^{-1}, consistent with the previously reported detection above $\sim$1 TeV for steady emission.

Key words: gamma rays: bursts – pulsars: individual: PSR 1706-44

1. Introduction

PSR 1706−44, discovered during a pulsar survey of the southern sky (Johnson et al. 1992), has a 102ms pulsar period and characteristic age of $\sim$17000 years. It is an isolated rotation powered pulsar and has been established as a source of X-rays and γ-rays up to TeV energies. The X-ray flux detected by the ROSAT satellite is unpulsed (Becker et al. 1995) with a 2σ upper limit to the pulsed fraction of 18%. Synchrotron radiation is favoured for the X-ray emission mechanism due to the lack of a pulsed component and similarity of pulsar parameters to those of the Vela pulsar (Becker et al. 1997).

High Energy (HE) γ-ray emission from PSR1706−44, first detected by the EGRET detector on-board the CGRO satellite (Thompson et al. 1992), is pulsed at the rotational period of the radio pulsar and characterised by a single pulse profile. More recent results from EGRET (Thompson et al. 1996) indicate a spectral break at 1 GeV. PSR1706−44 is one of only seven pulsars discovered as a source of HE γ-rays. An established trend between the pulsar characteristic age and pulsed HE γ-ray spectral index indicates that older pulsars are more efficient at emitting higher energy γ-rays (Thompson et al. 1994).

The ground-based Atmospheric Čerenkov Imaging (ACI) technique was pioneered by the Whipple group and led to their discovery of unpulsed TeV γ-rays from the Crab nebula (Vacanti et al. 1991 & Weekes et al. 1989). This technique images the optical Čerenkov radiation produced by extensive air showers (EAS) in the atmosphere to discriminate EAS initiated by γ-rays from those initiated by the far more numerous cosmic rays. The discrimination is based on a moment-based fit whereby images are approximated by ellipses, and implemented by making cuts on images properties or parameters. Further discussion is left to Sect. 2. Large mirrors are required ($\geq$4 m diameter) in order to obtain a sufficient Čerenkov signal to skynoise ratio and low energy threshold. Subsequent to the Whipple Crab discovery, vigorous efforts to utilise the ACI technique have resulted in a number of groups operating worldwide. Clear evidence of TeV γ-ray emission has been obtained for only a few sources to date: the galactic pulsars Crab nebula/pulsar and PSR 1706−44, and the active galactic nuclei Markarian 421 (Quinn et al. 1996) and Markarian 501 (Schubnell et al. 1996). The Vela Pulsar may also be established as a source of TeV γ-rays (Yoshikoshi et al. 1997).

PSR1706−44 was the first southern hemisphere source of TeV γ-rays detected by the Collaboration between Australia and Nippon for a Gamma Ray Observatory in the Outback (CANGAROO) (Kifune et al. 1995) using the ACI technique at Woomera, Australia. The flux $>$1 TeV from PSR1706−44 is calculated at 0.8×10^{-11} photons cm^{-2}s^{-1}, equating to a γ-ray luminosity of 3×10^{33} erg s^{-1} (at 1.5 kpc). This flux was found to be unpulsed (Kifune et al. 1995). These data were obtained with the 3.8 metre diameter reflector and an imaging camera of between 220 and 256 photomultiplier tube (PMT) pixels (Hara et al. 1993), with each pixel viewing a $0.^\circ12 \times 0.^\circ12$ area of sky. An earlier search for pulsed TeV emission by the Potchefstroom group in South Africa using the non-imaging timing method (Nel et al. 1993) was unsuccessful, and a 3σ upper limit 5.8×10^{-12} photons cm^{-2}s^{-1} above 2.6 TeV was set.

Send offprint requests to: G.P. Rowell
⋆ *Present address:* Institute for Cosmic Ray Research, University of Tokyo, Tokyo 188, Japan

Table 1. Observed and derived parameters of PSR1706−44. From Nicastro et al. (1996).

R.A.(J2000)	$17^h09^m\ 42^s.17 \pm 0^s.08$
Dec (J2000)	$-44^\circ\ 28'\ 57'' \pm 3''$
Period, P	102.4497 ms
Period derivative $\dot{P}$	93×10^{-15}s
Distance (from HI)	2.8 kpc
Distance (from DM)	1.8 kpc
Characteristic age	17450 yr

Models put forward to explain the unpulsed nature of TeV γ-rays in pulsar environments have centred on the boosting of photons by Inverse Compton (IC) scattering in regions more distant from the pulsar than those leading to HE γ-ray production. For PSR1706−44, IC scattering on the 2.7 K microwave background is suggested (Harding 1996) as the dominant mechanism over IC scattering on other photon sources (such as synchrotron photons), given the low magnetic field of the pulsar. A plerion or associated compact supernova remnant is implied by the steady X-ray emission.

In this work we present results from the second CANGAROO telescope, a 4 metre diameter reflector using a somewhat lower resolution camera of 37 pixels designed and built by the University of Adelaide. The BIcentennial Gamma Ray Telescope, BIGRAT, operates at a modal γ-ray energy roughly half that of the 3.8 metre telescope. We will briefly discuss the simulated performance of BIGRAT in the next section. Table 1 is a list of current pulsar parameters.

2. Experiment

The University of Adelaide has operated the BIGRAT since 1988. Currently, three segmented parabolic mirrors (4 metre diameter) are mounted on a single elevation-azimuth structure. An imaging camera of 37 photomultiplier (Hamamatsu R2102 13mm square PMT) pixels ($\sim$0.3° resolution) is mounted at the focus of the central mirror providing $\sim$2.3° field of view. Single PMTs (EMI 9822B 1.6°) are mounted at the foci of the outer mirrors. An event trigger is a triple coincidence between central camera pixels and both outer PMTs within a resolving time of $\sim$10 ns. The triple coincidence reduces the number of accidental triggers due to skynoise and unaccompanied muons. Data are taken using the ON-OFF source method, enabling a search for both unpulsed and pulsed emission from prospective sources. The ON source region is centred on the source of interest while the OFF source region is displaced in right ascension (RA) such that equal bands of elevation and observation times are covered in both runs. The AC-coupled PMT pulses arising from EAS are integrated over a $\sim$ 15ns window using LeCroy analogue to digital converters (ADCs) (Rowell et al. 1997) and the ADC outputs are recorded for all pixels for each event. Skynoise is also present in the PMT pulses and is a source of undesirable extra fluctuations in the ADC signal. In preliminary data processing ADC pedestals are subtracted from the ADC values for each camera pixel and a correction factor is applied to each pixel to account for differences in PMT gains. The ADC value for each pixel is then used as a weighting factor in the calculation of image parameters.

A drawback of the ON-OFF observation technique is that differences in skynoise can occur between ON and OFF source data, leading to biases in ON–OFF excesses after γ-ray selection cuts. A technique known as software padding (Cawley 1993) has been used to address this problem. However, we have found that modifications to this technique are necessary when analysing data from BIGRAT owing to the relatively low performance of the camera/mirror combination and large differences in skynoise found between ON and OFF source data, particularly when the ON source region lies at low galactic latitude and longitude. The software padding modifications are described in detail in Rowell et al. (1997). In that work we defined two software padding algorithms based on the asymmetry of skynoise ADC distributions:(1) Fixed asymmetric and (2) Variable asymmetric software padding. Both of these provide an improved equalisation of skynoise fluctuations below and *above* ADC pedestals. In these methods, an adjustment is made to compensate for the asymmetry of skynoise about ADC pedestals. This adjustment is fixed for all camera pixels in fixed asymmetric software padding, while in variable asymmetric software padding the adjustment is variable on a pixel-by-pixel basis depending on the level of skynoise found in a given pixel. Both forms of padding produced statistically similar results when applied to BIGRAT data. However, variable asymmetric software padding is considered an intuitively better solution for coping with large differences in skynoise across the camera.

An alternative to software padding is hardware padding which makes use of computer-stabilised light emitting diodes (LEDs) to add a controlled amount of noise to each PMT. Hardware padding is now considered suitable only in low to medium resolution cameras and often adds an unnecessary amount of extra noise to each Čerenkov image. Hardware padders were replaced by software padding at the end of the 1993 observing season for PSR1706–44. After software/hardware padding, image cleaning and a software trigger or re-trigger are applied to each image. In image cleaning, pixels are removed if they are suspected to be skynoise-dominated, while the re-trigger is designed to filter out images which have low maximum and/or total signal and therefore likely to be skynoise-dominated. In this work the re-trigger was the application of a lower limit on the most intense pixel in the image and any image not meeting this criterion was rejected.

Finally, the algorithms of Hillas (1985) are used to calculate image parameters in which the images are approximated by ellipses. γ-ray images will preserve the arrival direction of their primary γ-ray and thus their image major axes are expected to point to the camera field of view centre. This is not the case for cosmic ray images which will have essentially random orientations in the focal plane, reflecting their random arrival directions due to the influence of interstellar and intergalactic magnetic fields during transit. Also, physical differences between γ-ray and cosmic ray EAS allow discrimination based on image shape.

Table 2. Predicted quality factors for various image parameters based on Monte Carlo simulations of the 37 pixel camera using the optimal γ-ray selection criteria (γ-ray domain). Optimal thresholds for cleaning and re-triggers were applied. The percentages of γ-rays and cosmic rays surviving each cut are relative to those that trigger the camera, prior to the re-trigger. The errors in the quality factors are statistical.

Image Parameter	Q-factor	% γ-rays remaining	% Cosmic rays remaining	γ-ray domain
azwidth	2.6 ±0.4	48.8	3.5	$\leq$0.22°
length	2.4 ±0.3	46.2	3.8	$\leq$0.27°
conc2	2.0 ±0.2	49.1	5.9	$\geq$0.52
tnum	1.9 ±0.2	42.3	5.0	$\leq$9.0

The optimum thresholds for cleaning, re-triggering and γ-ray image discrimination were determined *a priori* by Monte Carlo simulations of the camera performance and were scaled with the level of skynoise for each pixel. The scaling ensured that the absolute thresholds of both processing steps follow the skynoise levels across the camera, which can be quite different owing to stars traversing the field of view.

3. Simulations

Simulations of Čerenkov images due to cosmic rays were created by using the species H, He and N in the ratio (1):(0.49):(0.40) according to Ichimura et al. (1993). Nitrogen was assumed to also represent fluxes from carbon, oxygen, sodium and magnesium. Iron was not included due to its low trigger efficiency. All shower energies were sampled from an integral power law starting at 0.5 TeV with spectral index -1.65. The minimum energy was low enough to enable the modal energy of detected γ-rays and cosmic rays to be determined. Image cleaning is implemented using two thresholds. Any pixel below the *rigid* threshold regardless of its location in an image is discarded. Any pixel less than the *isolated* threshold is discarded (i.e. set to zero) if and only if it is not adjacent to any pixel of intensity greater than or equal to the isolated threshold. The isolated threshold removes pixels of moderate intensity that are separated from the main image and the isolated threshold is greater than the rigid threshold.

A measure of camera performance was based on the imaging quality factor Q:

$$Q = \frac{N_\gamma}{N_\gamma^t}\left(\frac{N_{cr}}{N_{cr}^t}\right)^{-\frac{1}{2}} \quad (1)$$

where N_γ is the number of γ-rays surviving the cut, N_γ^t is the total number of γ-rays prior to the cut while N_{cr} and N_{cr}^t are the number of cosmic rays after and prior to the cut respectively. In Fig. 1 we show the quality factor contours for the four highest performing image parameters as a function of the isolated and rigid cleaning thresholds in combination with the re-trigger. *Conc2* is defined as the ratio of the brightest pair of adjacent pixels to the total signal in the image and *tnum* the number of non-zero pixels in an image. *Azwidth* is defined as the width of the image perpendicular to the line from the image centroid and the field of view centre while *length* is the length along the image major axis. *Azwidth* is a pointing parameter and in general we expect γ-ray images to have smaller *azwidth length* and *tnum* and higher *conc2* than those from cosmic rays. Mathematical descriptions for these parameters are given in Weekes et al. (1989).

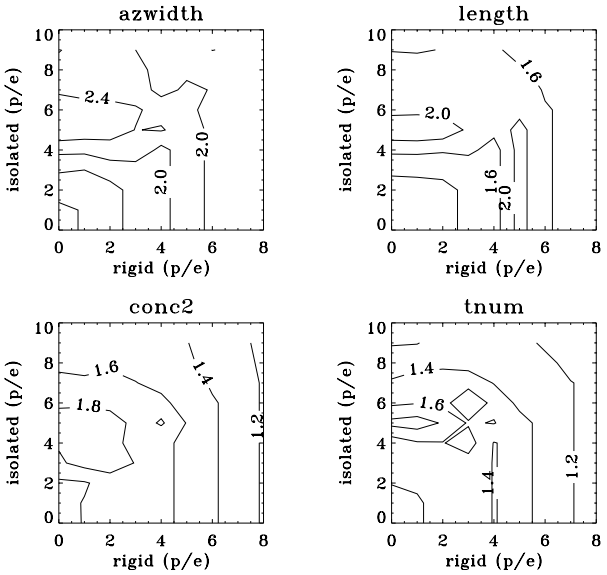

Fig. 1. Contour plots of imaging quality factor as a function of the two-dimensional cleaning strength. The figure shows the optimum values for the two cleaning thresholds. 'Rigid' is the rigid threshold and 'isolated' refers to the isolated pixel threshold, both in units of photoelectrons. A re-trigger is also used where an image is selected if its most intense pixel is greater than or equal to 14 photoelectrons.

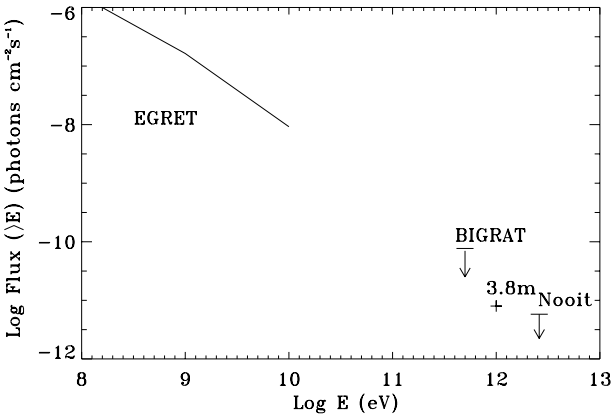

Fig. 2. Comparison of BIGRAT 3σ *azwidth* upper limit from this work with other measurements. The 3.8m (CANGAROO), Nooit (Nooitgedacht) and EGRET results are from Kifune et al. (1995) , Nel et al. (1993) and Thompson et al. (1996) respectively. Note that the EGRET and Nooitgedacht results are for pulsed emission only.

Optimum values for the isolated and rigid cleaning thresholds were found to be $\sim$5 photoelectrons and $\sim$1.5 photoelectrons respectively, based on the performances of *azwidth* and *length* parameters. The optimum re-trigger threshold was found

Table 3. Statistics for PSR1706−44 data from the 1993 and 1994 observing seasons. Selected events are from those ON–OFF pairs with RA separation $\leq$3 hrs and considered suitable for analysis. In the last row, a software-based re-trigger of 14 photoelectrons has been applied following variable asymmetric software padding. The excess significance was calculated using the statistics of Li & Ma 1983.

Data type	Time (hrs)	Events (ON)	Events (OFF)	Excess (σ)
Raw	93.7	796468	756337	+32.2
Selected	37.6	324104	320882	+4.0
Re-trigger	37.6	159524	158995	+1.2

Table 4. ON–OFF event excess at each γ-ray cut for the best four image parameters using the PSR1706−44 1993/1994 dataset. 3σ upper limits to the γ-ray flux >0.5 TeV are also included where the uncertainties are statistical.

Image parameter	ON	OFF	σ	3σ upper limit to flux (>0.5 TeV) photons cm^{-2} s^{-1}
azwidth	8476	8282	+1.5	$7.0(\pm0.7) \times 10^{-11}$
length	11730	11517	+1.4	$8.6(\pm0.8) \times 10^{-11}$
conc2	17492	17265	+1.2	$9.4(\pm0.8) \times 10^{-11}$
tnum	28164	27807	+1.5	$14.8(\pm1.5) \times 10^{-11}$

to be ∼14 photoelectrons. The final quality factor was calculated where N_{cr} and N_γ^t (Eq. 1) represented the original number of cosmic ray and γ-ray events prior to the re-trigger to enable a direct assessment of any improvement afforded by the re-trigger. Table 2 lists the optimum quality factors for each parameter and their respective selection criterion (γ-ray domain). The parameter *alpha* which is the angle between the image major axis and the image centroid to field of view centre is not well determined by the BIGRAT camera and was not used in analysis. *Alpha* is used by many groups using higher resolution cameras since it is less sensitive to systematic effects.

Using the laboratory measured conversion factor of ∼1.7 photoelectrons per ADC count, the optimal cleaning and re-trigger thresholds were applied to data as multiples of the measured skynoise fluctuations for Čerenkov data. Skynoise fluctuations were estimated by fitting a half Gaussian to the ADC distribution below pedestal for each pixel with the level of skynoise present being expressed as the standard deviation (in ADC counts) of the fitted half-Gaussian. The cleaning isolated and rigid thresholds correspond to 3.1σ and 0.6σ respectively where σ is the average skynoise fluctuation for the dataset. Similarly, the re-trigger threshold corresponds to $\sim 8\sigma$. The effective collecting area for γ-rays (>0.5 TeV) was calculated from simulations to be $1.18(\pm0.05) \times 10^8$ cm^{-2} s^{-1} based on the integral γ-ray trigger efficiency over the ground area in which the EAS were simulated (1.96×10^9 cm^2).

4. Results of data analysis

Observations of PSR1706−44 were made between May 1993 and October 1994 using the ON–OFF source method and a search for TeV γ-ray emission was carried out. The observation method is sensitive to both steady and pulsed emission although a pulsed search was not carried out here. A total of 104.8 and 93.7 hours were spent ON and OFF source respectively.

After the removal of poor quality data, caused, e.g., by the influence of cloud, a very large ON source raw excess in the ON–OFF matched data was obtained. Further investigation (Rowell 1995) revealed that the majority of the large ON source excess was found in data taken with a right ascension (RA) difference greater than 3 hours between ON and OFF source runs and these data were not considered for further analysis. Such large offsets in RA arose from efforts to maximise the stereo data taken with the 3.8 metre telescope. Stereo analyses are described in more detail elsewhere (Thornton et al. 1995). These data with RA offset greater than 3 hours were found to be under the influence of a systematic change in observation conditions. This step removed over half of the raw data, but was necessary to ensure the data being considered were free from contamination. Table 3 summarises the PSR1706−44 dataset where selected events are those ON, OFF pairs with RA separation $\leq$3 hours. For these data, the skynoise found ON source was on average $\sim$ 2% greater than that OFF source, and the ON source excess can be attributed to this difference. The excess significances were calculated using the statistics of Li & Ma (1983). Re-trigger events are those surviving the software-based re-trigger discussed earlier used in conjunction with variable asymmetric software padding. Variable asymmetric software padding was applied to equalise skynoise in ON–OFF data and the resulting excess at each image parameter cut was calculated. In Table 4 we give the resulting excess for various image parameters. For all parameters, the ON–OFF excess is less than 3σ and therefore there is no compelling evidence for the detection of VHE γ-rays. Upper limits were obtained for the above excesses using the method of Protheroe (1984). The 3σ upper limit to the steady flux of TeV γ-rays for each cut was calculated assuming that the excess after dividing by the cut efficiency predicted for each image parameter is due entirely to γ-rays.

5. Discussion and conclusions

PSR1706−44 data taken with the University of Adelaide's Čerenkov imaging telescope (BIGRAT) have been analysed for a steady flux of TeV γ-rays above 0.5 TeV. No evidence for TeV γ-ray emission was seen and 3σ upper limits to the flux were calculated. A comparison with other γ-ray detections is given in

Fig. 2 where we include the upper limit derived from the *azwidth* cut incorporating the statistical uncertainty (i.e. 7.7×10^{-11} photons cm^{-2} s^{-1}). We find that the upper limit from this work is consistent with the steady flux reported by Kifune et al. (1995) at a higher energy. A lower limit on the integral spectral slope for the TeV emission from the *azwidth* parameter is calculated at -3.3 when combined with the Kifune result, and perhaps indicates that the spectrum does not steepen sharply in going from GeV to TeV energies.

Further data has been taken during 1995 and 1996 with the requirement that the maximum RA separation between ON and OFF source be $\leq$3 hours and analysis of these data is underway. Enhancements to the BIGRAT camera have also been completed with a further 57 pixels being added and expanding the field of view to $\sim3.2^\circ$ (Dazeley et al. 1997).

Acknowledgements. This work is supported by grants from the Australian Research Council. GPR, GJT and PGE acknowledge receipt of Australian Research Council Fellowships during the course of this work.

References

Becker W., Brazier K.T.S., Trümper J. 1995, A & A 298, 528.
Becker W., Trümper J. 1997, A & A 236, 682.
Cawley M. 1993, in '"Towards a Major Atmospheric Cerenkov Detector" II (Calgary)', p. 176.
Dazeley S.A., Patterson J.R., Rowell G.P. 1997, Proc 25th ICRC (Durban) 5, 137.
Hara T., Kifune T., Matsubara Y. et al. 1993, Nucl Inst Meth A332, 300.
Harding A. 1996, Space Sci Rev 75, 257.
Hillas A. 1985, Proc 19th ICRC (La Jolla) 3, 445.
Ichimura M., Kamioka E., Kirii M. et al 1993, Proc 23rd ICRC (Calgary) 2, 5.
Johnson S., Lyne A.G., Manchester R.N. et al 1992, MNRAS 255, 401.
Kifune T., Tanimori T., Ogio S. et al 1995, ApJ 438, L91.
Li T., Ma Y. 1983, ApJ 272, 317.
Nel H.I., de Jager O.C., Raubenheimer B.C. et al. 1993, ApJ 418, 836.
Nicastro L., Johnson S., Koribalski B. 1996, A & A 306, L49.
Protheroe R. 1984, Astron Express 1, 33.
Quinn J. Akerlof C.W., Biller S. et al. 1996, ApJ 456, L83.
Rowell G.P. 1995, PhD thesis, The University of Adelaide.
Rowell G.P., Edwards P.G., Patterson J.R., Thornton G.J. 1997, Astro Part Phys 7, 35.
Schubnell M.S., Akerlof C.W., Biller S. et al. 1996, ApJ 460, 644.
Thompson D.J., Bertsch J.A., Esposito J.A. et al 1996, ApJ 465, 385.
Thompson D.J., Arzoumanian Z., Bertsch D.L. et al. 1992, Nat 359, 615.
Thompson D.J., Arzoumanian Z., Bertsch D.L. et al. 1994, ApJ 436, 229
Thornton G.J., Dazeley S.A., Edwards P.G. et al. 1995, Proc 24th ICRC (Rome) 3, 476
Vacanti G., Cawley M.F., Colombo E. et al. 1991, ApJ 377, 467.
Weekes T.C., Cawley M.F., Fegan D.J. et al. 1989, ApJ 342, 379.
Yoshikoshi T., Kifune T., Dazeley S.A. et al. 1997, ApJ 487, L65.

This article was processed by the author using Springer-Verlag LaTeX A&A style file *L-AA* version 3.